

Effects of a floating wave barrier with square cross section on the wave-induced forces exerted to an offshore jacket structure

Arash Dalili Osgouei¹, Ramin Vafaei Poursorkhabi^{*2},
Ahmad Maleki¹ and Hamid Ahmadi^{3,4}

¹Department of Civil Engineering, Maragheh Branch, Islamic Azad University, Maragheh, Iran

²Department of Civil Engineering, Tabriz Branch, Islamic Azad University, Tabriz, Iran

³Faculty of Civil Engineering, University of Tabriz, Tabriz 5166616471, Iran

⁴Center of Excellence in Hydroinformatics, Faculty of Civil Engineering, University of Tabriz, Tabriz, Iran

(Received March 8, 2021, Revised August 16, 2021, Accepted September 3, 2021)

Abstract. The main objective of the present research was investigating the effects of a floating wave barrier with square cross section installed in front of an offshore jacket structure on the wave height, base shear, and overturning moment. A jacket model with the height of 4.55 m was fabricated and tested in the 402 m-long wave flume of NIMALA marine laboratory. The jacket was tested at the water depth of 4m subjected to the random waves with a JONSWAP energy spectrum. Three input wave heights were chosen for the tests: 20 cm, 23 cm, and 28 cm. Results showed that the average decrease in the jacket's base shear due to the presence of a floating wave barrier with square cross section was 18.97%. The use of wave barriers with square cross section also resulted in 19.78% decrease in the jacket's overturning moment. Hence, it can be concluded that a floating wave barrier can significantly reduce the base shear and overturning moment in an offshore jacket structure.

Keywords: base shear; floating wave barrier; jacket structure; NIMALA wave flume; overturning moment; random waves

1. Introduction

The jacket-type platform is the most common offshore structure employed for the oil and gas production from the reservoirs below the seabed. It consists of three main parts: superstructure or topside, substructure or jacket, and the foundation or piles. Jacket substructure is a steel space frame fabricated by welding the thin-walled circular hollow section (CHS) members, also called tubulars.

Construction of floating breakwaters and wave barriers is one of the commonly used methods for the protection of harbors and coastal structures. However, their application for the protection of offshore structures has not been extensively studied (Asgari Motlagh *et al.* 2021). The present paper investigates the effects of a floating wave barrier installed in front of an offshore jacket structure on the wave height, wave-induced forces, and consequently jacket's base shear and overturning moment.

The calculation of forces exerted to tubular structures, such as a jacket substructure, due to the random sea waves has an extensive history including experimental, numerical, and theoretical

*Corresponding author, Ph.D., E-mail: raminvafaei@yahoo.com

studies. Several studies have been conducted in regards to the wave force effect on slender bodies, for various loading cases. One of the most famous studies on the wave forces applied to cylindrical piles was the one conducted by Morison *et al.* (1950) in which the in-line wave force was assumed to be the linear sum of two components: drag force and inertia force. Chan *et al.* (1995) studied the plunging wave impacts on vertical cylinders. Goda *et al.* (1966) investigated the impulsive breaking wave forces on piles. Murgoitio *et al.* (2020) studied the impact forces of nearly breaking waves on vertical circular cylinders. Hildebrandt (2013) investigated the hydrodynamic of breaking waves on offshore wind turbine structures. Sruthi and Sriram (2017) studied the wave impact load on jacket structure in intermediate water depth.

Various aspects of the behavior of floating breakwaters and wave barriers subjected to sea waves have been investigated by previous researchers. Sannasiraj *et al.* (1998) investigated the mooring forces and motion responses of pontoon-type floating breakwaters. Abul-Azm and Gesraha (2000) studied the hydrodynamics of floating pontoons under oblique waves. Gesraha (2006) analyzed the shaped floating breakwater in oblique waves. Rahman *et al.* (2006) presented a numerical modeling for the estimation of dynamic responses and mooring forces of submerged floating breakwaters. Dong *et al.* (2008) carried out a number of experiments on the wave transmission coefficients of floating breakwaters. Zhao *et al.* (2012) investigated the interaction between waves and an array of floating porous circular cylinders. Tsai *et al.* (2016) developed a novel control algorithm for interaction between surface waves and a permeable floating structure. Christensen *et al.* (2018) conducted a set of experimental and numerical studies on floating breakwaters. Ji *et al.* (2018) studied the interactions between free-surface waves and a floating breakwater with cylindrical-dual/rectangular-single pontoon using numerical and experimental techniques. Nikpour *et al.* (2019) conducted an experimental study on wave attenuation in trapezoidal floating breakwaters.

Base shear and overturning moment are two crucial parameters for the analysis and design of offshore jacket structures subjected to random wave loading. Although majority of the research conducted on the estimation of these two parameters are numerical investigations (Jusoh 2021, Chakrabarty 2005), present paper focuses on the large-scale experimental study of jacket's behavior under random wave-induced forces. In the present research, a jacket model with the height of 4.55 m was fabricated and tested in wave flume of NIMALA marine laboratory. The wave flume was 402 m long. The jacket was tested at the water depth of 4m subjected to JONSWAP waves with the input wave height of 20 cm, 23 cm, and 28 cm. The mechanism of wave energy dissipation due to hitting a wave barrier is mainly a combination of the wave diffraction and the wave reflection. A square cross section was selected for the wave barrier.

2. Details of experimental study

2.1 Wave-maker flume

Experiments of the present research were conducted in NIMALA marine laboratory. Its wave flume, that is the biggest one in Iran, is 402 m long, 6 m wide, and 4.5 m high (Fig. 1). The water depth in the flume was 4 m. NIMALA lab has ISO/IEC 17095 2005 and ISO 9001:2015 certificates (NIMALA, 2018). The installation, setup, and calibration of equipment were accomplished according to the ITTC documents (ITTC, 2008).

Wave-maker paddle that is of the piston type is capable of generating regular and random waves having the frequency content of Bretschneider, Pierson-Moskowitz (P-M), and JONSWAP wave



Fig. 1 Wave flume and manned chariot of NIMALA marine laboratory

spectra. The maximum wave height that can be achieved by its wave maker is 50 cm.

Wave probes, which are of the resistance sensor type, are connected to a data logging system through an amplifier. They are capable of recording the time series of the water surface level with high accuracy. The wave flume has a 7.6 mX7.0 m manned chariot with the speed range of 0.5–10 m/s.

The wave absorber at the end of the flume is fabricated by reticulated panels in order to minimize the wave reflection and to avoid the interference between the incident and reflected waves. However, since the flume is quite long and the duration of each experiment was relatively short, data recording was usually done before the waves reach the flume end and consequently the wave reflection was generally not an issue.

2.2 Models of jacket structure and floating wave barrier

The jacket structure studied in the present research was a scaled model of C13 jacket installed in the South Pars gas field of the Persian Gulf. The height of the actual jacket is 80 m operating at the water depth of 72m. With a scale factor of 1 to 18, the model of the jacket was 4.4 m high installed in the flume at the water depth of 4m. The distance between the jacket and the wave maker was 70 m; while its distance from the flume end was 332 m. Fig. 2 shows the isometric view of the jacket structure.

As an idea to reduce the wave energy, a floating wave barrier was installed in front of the jacket structure. A square cross section was selected for the wave barrier. The material used for the fabrication of wave barrier was polystyrene. Since its specific weight is quite low, almost 98% of the wave barrier's cross section was above the water surface level when it was allowed to be floated freely.

A set of weights was attached to each wave barrier in order to ballast it to a position in which 50% of its cross section lies beneath the water surface level; i.e., to set its draft equal to half of its total height. The wave barriers were 5 m long having a 30 cmX30 cm cross section. There was a 50 cm gap between each barrier end and the adjacent flume wall. The wave barrier was located at the distances of 3 m and 5 m from the wave probes and the jacket structure, respectively.

Fig. 3 illustrates the longitudinal section of the wave flume along with the jacket structure and the equipment. Fig. 4 shows the dry jacket structure (Fig. 4(a)), the jacket installed in the flume without the wave barrier (Fig. 4(b)), and the jacket in the flume with the square-section wave barrier (Fig. 4(c)).

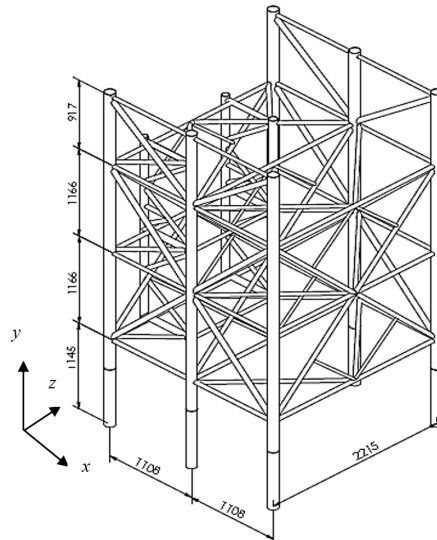


Fig. 2 Isometric view of the jacket model (unit: mm)

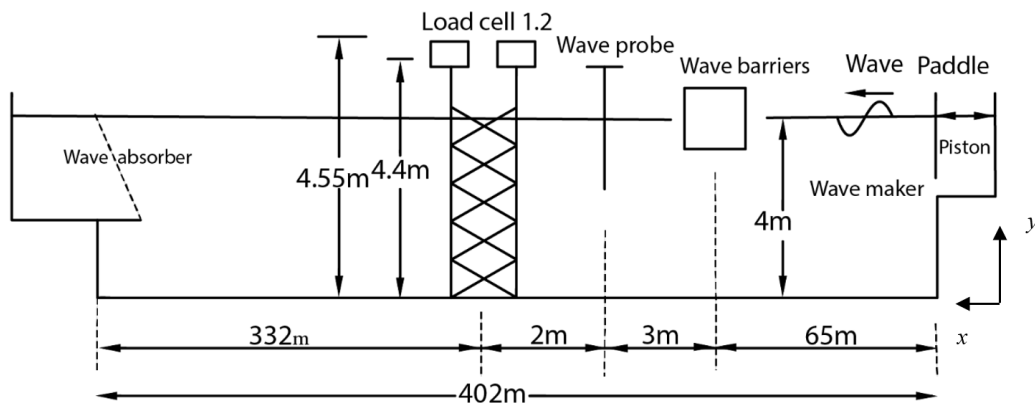


Fig. 3 Longitudinal section of the wave flume along with the jacket, wave barrier, and the equipment

2.3 Data recording and interpretation

The experiments were conducted in two phases: the jacket without the wave barrier and the jacket with the square-section wave barrier. In each phase, three sets of recording were done to determine the water surface level, base shear, and overturning moment of the jacket structure.

Water surface level was measured using resistance-type wave probes and the still water level (SWL) was set as the datum. The wave probes were installed between the jacket and the wave maker at a distance of 2 m from the jacket. The time step between the recorded data was 0.05s. Hence, 8000 levels were recorded during a 400s experiment. Considering the accurate calibration of the wave probes and the load cells, the recording of the force data was also done with 0.05s time steps. Load cells, which were the product of Wonbang Forcotech, had the force measurement capacity of 400N and 50N in the longitudinal and lateral directions, respectively (Fig. 5).

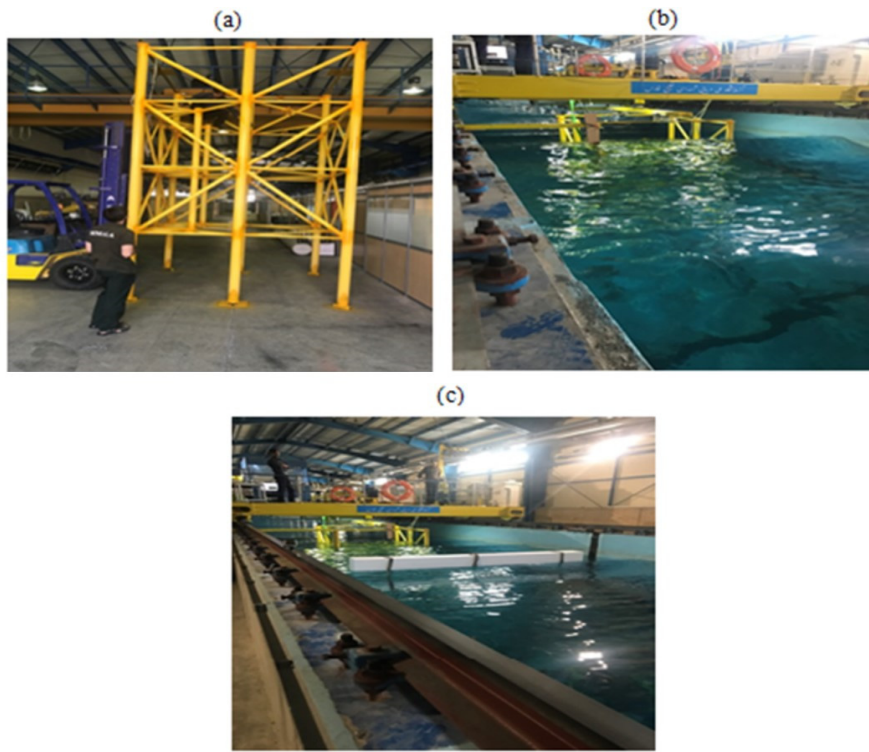


Fig. 4 (a) Dry jacket structure, (b) the jacket installed in the flume without the wave barrier and (c) the jacket in the flume with the square-section wave barrier



Fig. 5 Load cells used in the present research to measure the wave forces

Since the exerted force during an extreme wave was predicted to be larger than the capacity of a single load cell, two load cells were used to make sure that the total wave force would be recorded accordingly. The correlation between the two load cells was crucial. Hence, they were calibrated in such a way that there was no phase lag between their records.

The load cells were installed at the top of the structure instead of its bottom in order to ease the access and control during the successive experiments (Fig. 6(a)). Obviously, the base shear of the jacket structure would be equal to the total force recorded by the load cells (Fig. 6(b)). Assuming a pin support at the bottom of the jacket model, the overturning moment can be calculated as $F_{LC}h$; where F_{LC} is the total wave force recorded by the load cells and h is the jacket height (4.4 m) plus the height of the load cell position relative to the jacket top (0.15 m), i.e., $h = 4.55$ m (Fig. 6(c)).

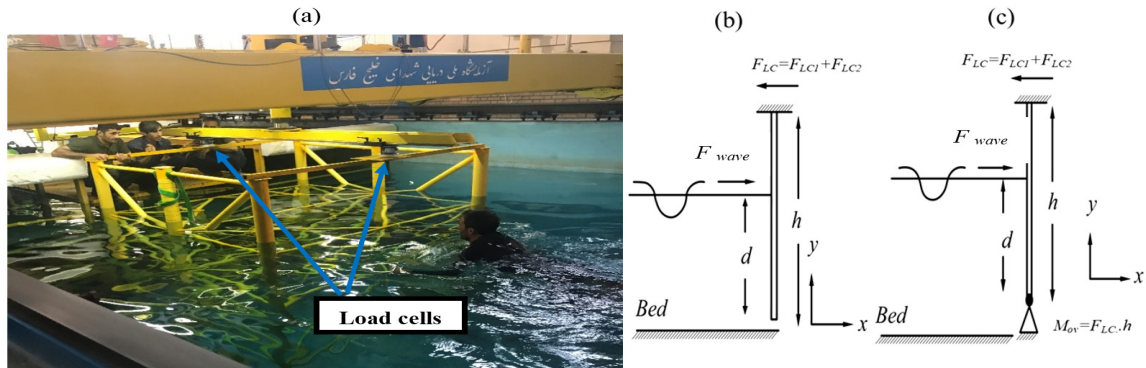


Fig. 6 (a) Installation of load cells, (b) Base shear (F_{BS}) recording mechanism and (c) Overturning moment (M_{ov}) recording mechanism

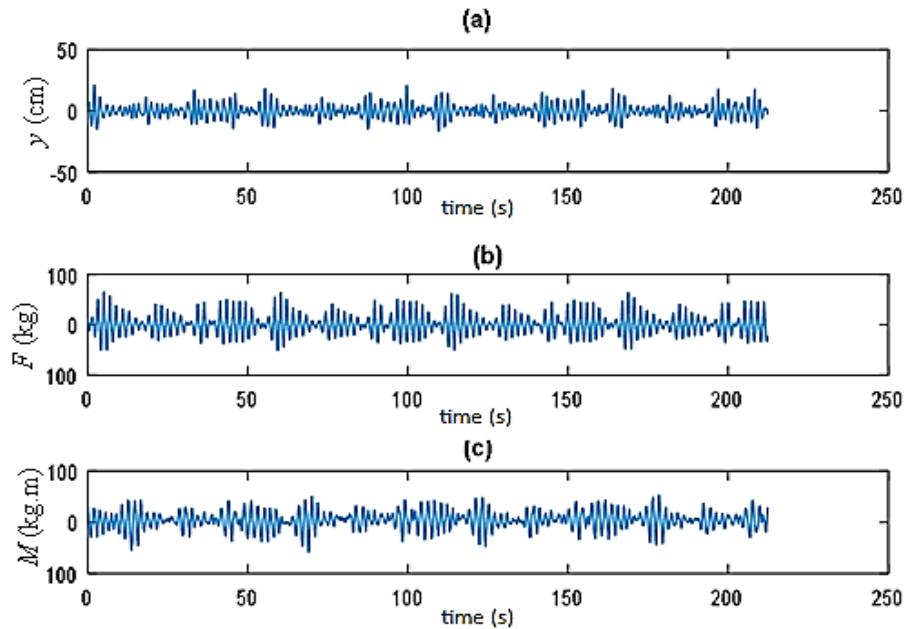


Fig. 7 Sample time series of recorded data: (a) Water surface level, (b) Base shear and (c) Overturning moment

3. Results and discussion

3.1 Dealing with recorded time series

Recorded time series of water surface level were used to determine the properties of individual successive waves. In order to do so, a MATLAB code was developed to employ the zero-up-crossing method for the calculation of individual wave heights and periods. Extracted data was then used to calculate the maximum wave height (H_{max}), significant wave height (H_s), mean wave height (H_{av}), maximum wave period (T_{max}), significant wave period (T_s), and mean wave period (T_{av}) along with the corresponding values of the wave length and wave frequency.

Table 1 Details of all experiments conducted during the present research

Base shear recording tests				
Jacket without the wave barrier	Wave-maker input wave height (cm)	20	23	28
	Wave condition	Nonbreaking	Nonbreaking	Nonbreaking
	Test ID	FN20	FN23	FN28
Jacket with the square-section wave barrier	Wave-maker input wave height (cm)	23		
	Wave condition	Nonbreaking		
	Test ID	FS23		
Overturning moment recording tests				
Jacket without the wave barrier	Wave-maker input wave height (cm)	20	23	28
	Wave condition	Nonbreaking	Nonbreaking	Nonbreaking
	Test ID	MN20	MN23	MN28
Jacket with the square-section wave barrier	Wave-maker input wave height (cm)	23		
	Wave condition	Nonbreaking		
	Test ID	MS23		

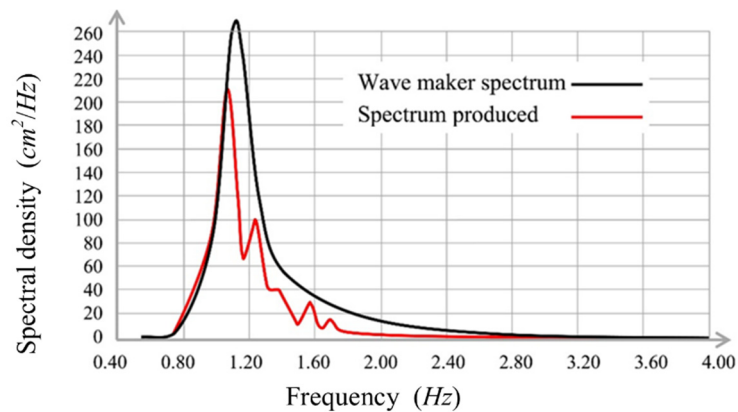


Fig. 8 The wave energy spectrum obtained from the generated waves (Red) and the JONSWAP spectrum used as the input for the wave maker (Black)

The degree of agreement between the wave energy spectrum obtained from the generated waves and the JONSWAP spectrum used as the input for the wavemaker depends on the precision of measurement sensors and the duration of wave making and full agreement is rather difficult to obtain. Such differences between the two spectrums is inevitable and quite normal.

There was a good agreement between the wave energy spectrum obtained from the generated waves and the JONSWAP spectrum used as the input for the wave maker (Fig. 8). The obtained spectrum, shown as an example in Fig. 8, is from the experiment conducted for determining the base shear of the jacket without the wave barrier in which $H_{w-in} = 28\text{cm}$, $T_{w-in} = 1.8\text{s}$, and $f_{w-in} = 0.56\text{ Hz}$.

The highest individual wave extracted from this experiment by the developed MATLAB code is depicted in Fig. 9 as an example. All the extracted wave heights are shown in Fig. 10 and the complete set of calculated wave properties is given in Table 2.

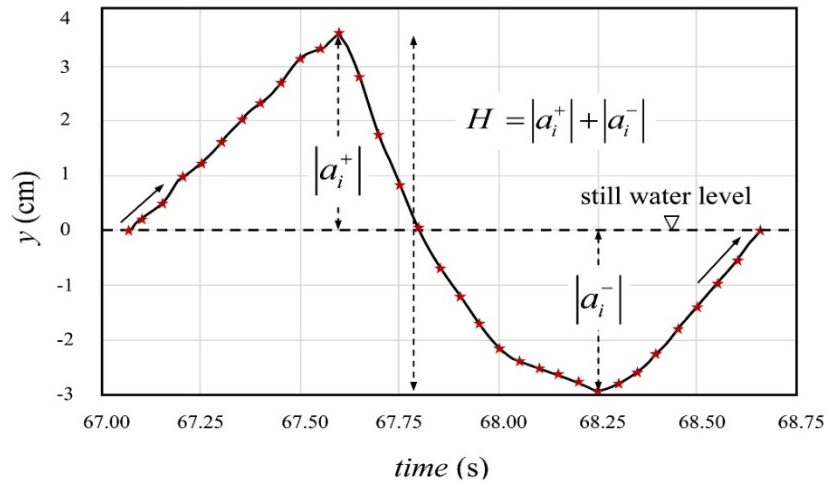


Fig. 9 The highest individual wave extracted by the developed MATLAB code from the experiment conducted for determining the base shear of the jacket without the wave barrier ($H_{w-in} = 28$ cm, $T_{w-in} = 1.8$ s, and $f_{w-in} = 0.56$ Hz)

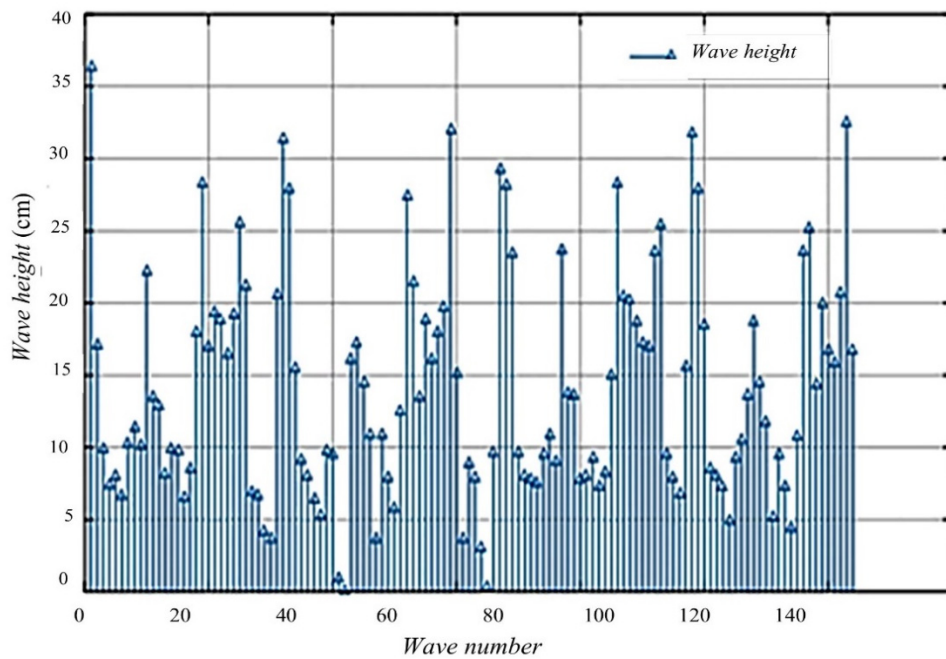


Fig. 10 Wave heights extracted from the experiment conducted for determining the base shear of the jacket without the wave barrier ($H_{w-in} = 28$ cm, $T_{w-in} = 1.8$ s, and $f_{w-in} = 0.56$ Hz)

The duration of wave generation was 250s. After the signal processing using MATLAB, 124 individual waves were obtained. Previous experiences of the corresponding author during an experimental study of wave forces on seawalls confirms the adequacy of the number of incident waves.

Table 2 The complete set of calculated wave properties from the experiment conducted for determining the base shear of the jacket without the wave barrier ($H_{w-in} = 28$ cm, $T_{w-in} = 1.8$ s, and $f_{w-in} = 0.56$ Hz)

Wave characteristic	Symbol	Value
Wave-maker input wave height	H_{w-in}	28 cm
Wave-maker input wave period	T_{w-in}	1.8s
Number of waves	N	124
Maximum wave height	H_{max}	36.31 cm
Significant wave height	H_s	26.21 cm
Mean wave height	H_{av}	14.03 cm
Maximum wave period	T_{max}	2.37s
Mean wave period	T_{av}	2.07s
Significant wave period	T_s	1.68s

Table 3 Data extracted from FN28 experiment

Wave length formula	L_{max} (m)	L_s (m)	L_{av} (m)
Finite water depth	1.8	1.74	0.52
d/L	2.22 OK.	2.29 OK.	7.69 OK.

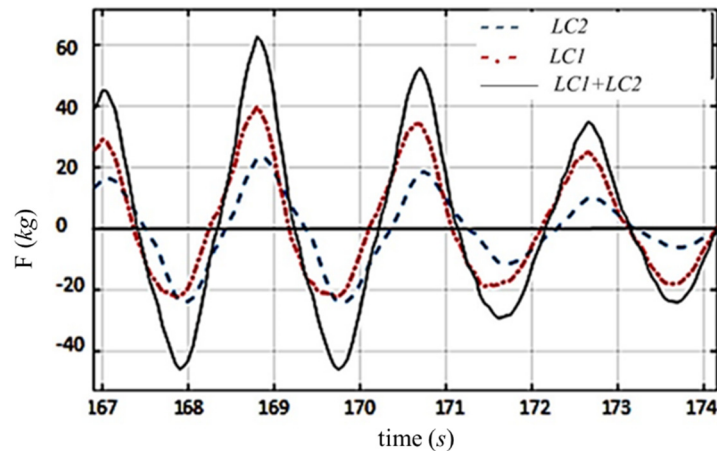


Fig. 11 The base shear of jacket structure as the sum of the forces recorded by the two load cells

The values obtained for the mean wave length (L_{av}), significant wave length (L_s), and the maximum wave length (L_{max}) showed that, in all experiments, the deep-water condition ($d/L > 0.5$) was completely satisfied for the L_{av} and L_s values; while it was nearly met for L_{max} values (Table 3). The depth of water in the wave flume (d) is 4 m.

The correlation between the two load cells was satisfactory and there was almost no phase lag between their records. Hence, the addition of the forces recorded by these two load cells would lead to the total wave force that was in fact the base shear of the jacket structure (Fig. 11).

When the water surface level on the jacket structure was above the SWL, the values recorded by the load cells were positive meaning that the force exerted to the structure was compressive; and

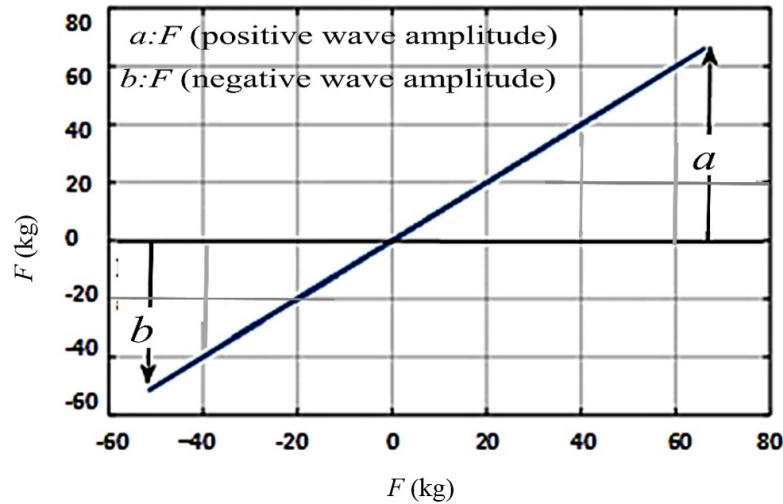


Fig. 12 The comparison of compressive and tensile wave forces exerted to the jacket structure

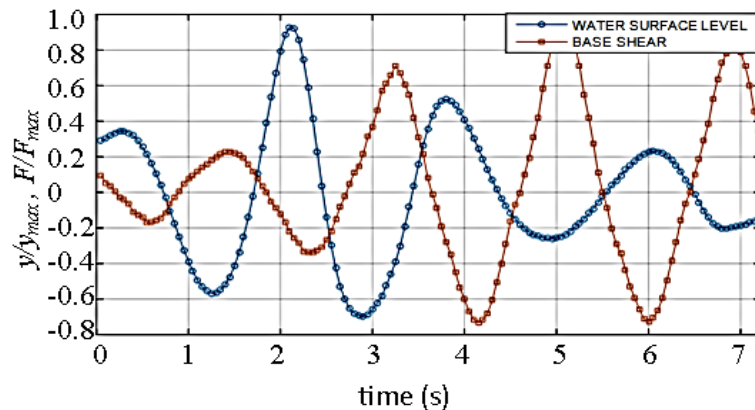


Fig. 13 Time series of relative water surface level and base shear as dimensionless parameters

when the water surface level on the structure was below the SWL, the recorded values were negative implying that the exerted force was tensile. The maximum compressive force was observed when the wave crest hit the jacket; and the maximum tensile force was recorded when the wave trough was on the structure. The maximum compressive forces were larger than the tensile ones as it was expected (Fig. 12). On an average basis for all the experiments, the difference between the maximum compressive and tensile forces was approximately 10%.

If one compared the time histories of relative water surface level and base shear as dimensionless parameters, a phase lag could be easily detected between them (Fig. 13). The reason was the 2m horizontal distance between the wave probe recording the water surface level and the load cells recording the base shear (Fig. 3). If we wanted to inspect the base shear due to the corresponding water surface level and wave height rigorously, this spurious phase lag must be eliminated. If the time series of the water surface level was being shifted forward as much as 20 data records, a satisfying correspondence would be achieved between the water surface level and the base shear.

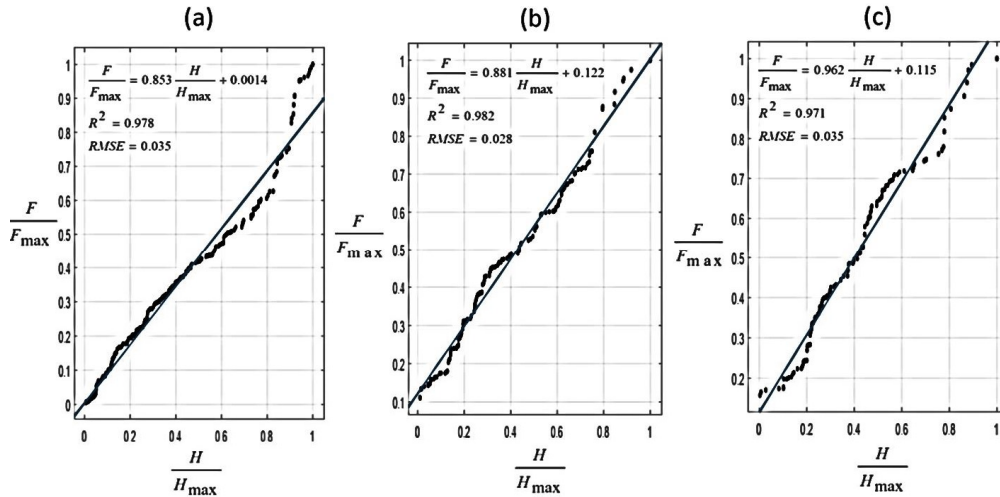


Fig. 14 The change of relative base shear (F/F_{max}) due to the change of relative wave height (H/H_{max}): (a) $H_{w-in} = 20$ cm, (b) $H_{w-in} = 23$ cm, (c) $H_{w-in} = 28$ cm

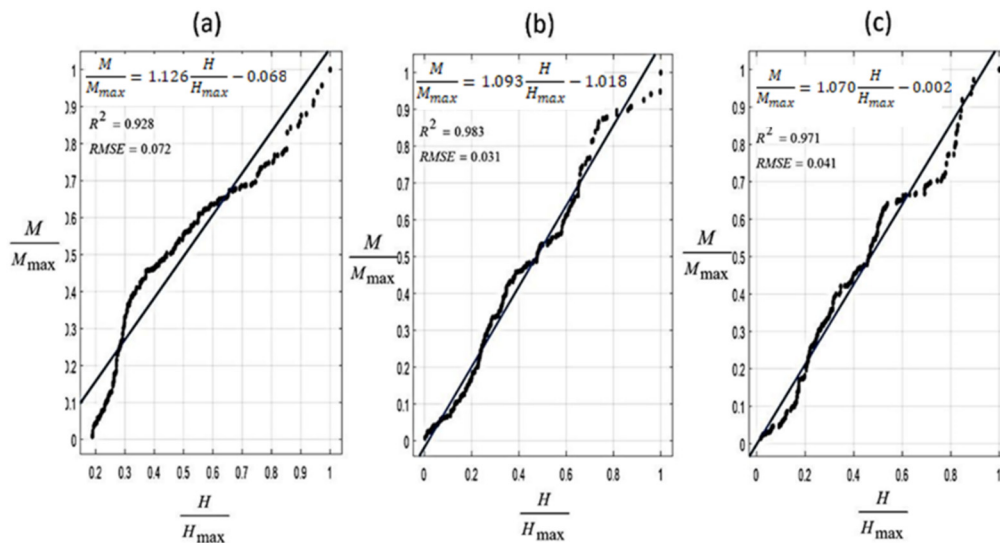


Fig. 15 The change of relative overturning moment (M/M_{max}) due to the change of relative wave height (H/H_{max}): (a) $H_{w-in} = 20$ cm, (b) $H_{w-in} = 23$ cm, (c) $H_{w-in} = 28$ cm

Considering the recording frequency of 0.05 Hz, a 20-record shift means a 1s phase shift in the time history of the water surface level. In fact, the 2m distance between the wave probe and the load cells led to a 1s time difference between their recordings. The same procedure was applied to the time series of water surface level when the overturning moment was being studied.

3.2 Jacket structure without a wave barrier

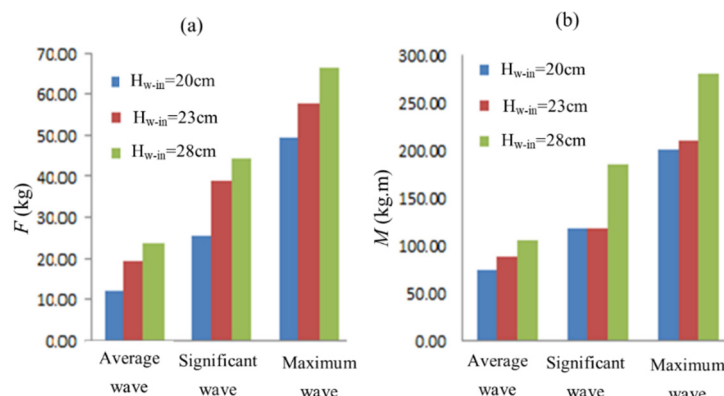
Figs. 14 and 15 show the change of relative base shear (F/F_{max}) and relative overturning moment (M/M_{max}) due to the change of relative wave height (H/H_{max}) for $H_{w-in} = 20$, 23, and 28 cm. H is the

Table 4 Values of the wave height, wave period, base shear, and overturning moment extracted from the experiments conducted on the jacket without the wave barrier

Test ID	H (cm)				T (s)		F (kg)			M (kg.m)		
	H_{w-in}	H_{av}	H_s	H_{ma}	T_{w-in}	T_{av}	F_{av}	F_s	F_{max}	M_{av}	M_s	M_{max}
FN20	23	7.90	16.00	23.36	18	1.15	12.11	25.48	49.38			
FN23	23	11.1	19.6	29.26	18	1.49	19.25	38.96	57.68			
FN28	28	14.0	23.2	36.39	18	1.65	23.82	44.48	66.29			
MN20	20	10.0	16.1	25.01	18	1.21				73.52	118.11	200.33
MN23	23	11.1	19.6	31.71	18	1.51				88.36	138.27	211.02
MN28	28	14.3	23.4	37.31	18	1.61				105.37	185.00	281.32

Table 5 The unknown coefficients of Eqs. (1)–(6) calculated based on the regression analysis of the data extracted from the experiments conducted on the jacket without the wave barrier

Test ID	Eq. (1)				Eq. (2)				Eq. (3)			
	a_1	b_1	R^2	RMSE	a_2	b_2	R^2	RMSE	a_3	b_3	R^2	RMSE
FN20	1.80	0.20	0.97	1.756	0.85	0.01	0.97	0.03	48.37	0.41	0.97	3.56
FN23	1.73	7.03	0.98	1.63	0.88	0.12	0.98	0.02	28.22	5.14	0.98	1.19
FN28	1.75	7.64	0.97	2.36	0.96	0.11	0.97	0.03	17.32	2.76	0.97	0.85
Test ID	Eq. (4)				Eq. (5)				Eq. (6)			
	a'_1	b'_1	R^2	RMSE	a'_2	b'_2	R^2	RMSE	a'_3	b'_3	R^2	RMSE
MN20	9.16	-3.78	0.91	4.69	1.12	-0.06	0.92	0.07	1309.00	-134.60	0.92	143.50
MN23	7.27	-3.76	0.98	6.61	1.09	-0.01	0.98	0.03	1066.00	-24.19	0.98	42.52
MN28	8.05	-0.55	0.97	11.06	1.07	-0.01	0.97	0.04	497.70	-1.13	0.97	27.66

Fig. 16 The change of the (a) base shear and (b) overturning moment due to the change of the wave height (calculated based on regression formulas obtained from Figs. 14 and 15 using H_{av} , H_s , and H_{max} as input)

recorded individual wave height, and F and M are the corresponding recorded base shear and overturning moment, respectively.

Recorded data presented in Table 4 was used to develop a set of equations expressing the relationships between the wave height and base shear/overturning moment. Following forms were

Table 6 The percentage of decrease in the base shear and overturning moment due to the decrease of the wave height

	Decrease of base shear (%)			Decrease of overturning moment (%)		
	Mean	Significant	Maximum	Mean	Significant	Maximum
Decrease of the wave maker input wave height from 28 cm to 23 cm	23.74	14.17	14.93	19.26	33.79	33.31
Decrease of the wave maker input wave height from 28 cm to 20 cm	96.70	74.57	34.24	43.32	56.63	40.43
Decrease of the wave maker input wave height from 23 cm to 20 cm	58.96	52.90	16.81	20.17	17.06	5.34

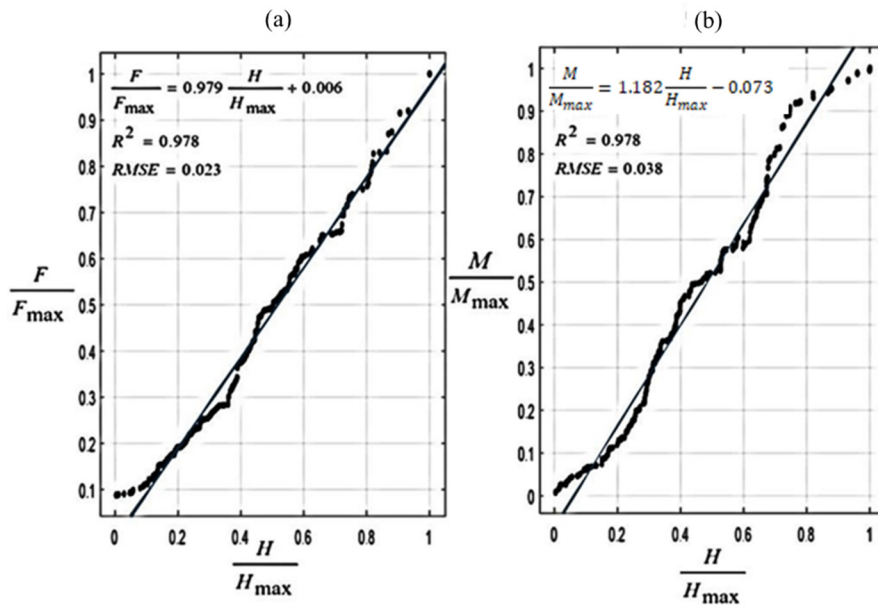


Fig. 17 The change of (a) relative base shear (F/F_{max}) and (b) relative overturning moment (M/M_{max}) due to the change of relative wave height (H/H_{max}) in the presence of a square-cross-section wave barrier

suggested for the formulas and the unknown coefficients calculated based on the regression analysis are given in Table 5. High coefficient of determination (R^2) values indicated the accuracy of regression analyses.

$$F = a_1H + b_1 \tag{1}$$

$$F/F_{max} = a_2(H/H_{max}) + b_2 \tag{2}$$

$$F/(\rho g H_{av}^3) = a_3(H/gT_{av}^2) + b_3 \tag{3}$$

$$M = a'_1H + b'_1 \tag{4}$$

$$M/M_{max} = a'_2(H/H_{max}) + b'_2 \tag{5}$$

$$M/(\rho g H_{av}^4) = a'_3(H/gT_{av}^2) + b'_3 \tag{6}$$

Fig. 16 along with Table 6 depict the percentage of reductions in the base shear and overturning moment due to reducing the wave height.

3.3 Jacket structure with a square-cross-section wave barrier

Fig. 17 shows the change of relative base shear (F/F_{\max}) and relative overturning moment (M/M_{\max}) due to the change of relative wave height (H/H_{\max}). Recorded data presented in Table 7 was used to develop a set of equations expressing the relationships between the wave height and base shear/overturning moment in the forms of Eqs. (1)-(6). The unknown coefficients calculated based on the regression analysis are given in Table 8.

Fig. 18 along with Table 9 depict the percentage of reductions in the base shear and overturning moment due to the presence of a floating wave barrier with a square cross section. It can be seen that, when the significant wave height is considered, the square-cross-section wave barrier has led to 18.97% and 19.78% reduction in the jacket's base shear and overturning moment, respectively.

It is worth mentioning here that, as can be observed in Table 9, the effect of the wave barrier on reducing the base shear and overturning moment is more highlighted in the case of higher waves. The reason is that the wave energy is a function of the square of the wave height.

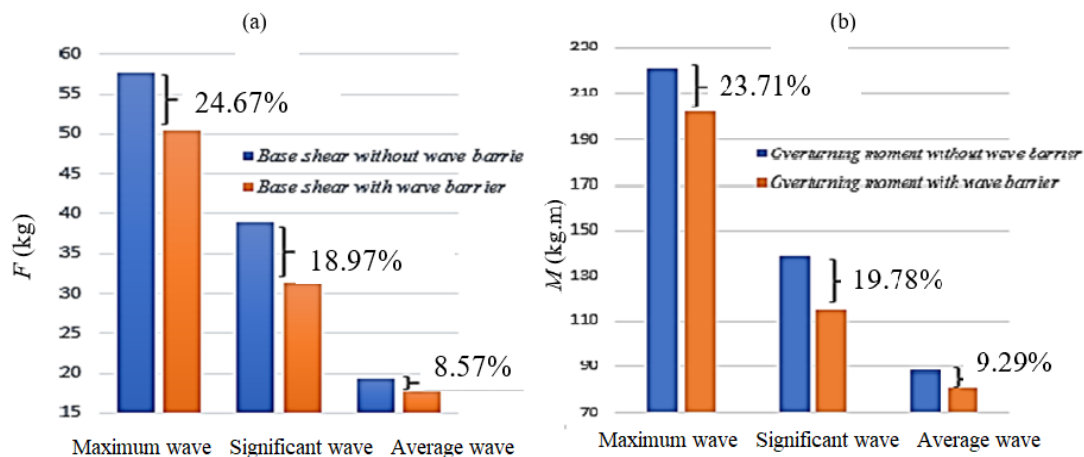


Fig. 18 The reduction of the (a) base shear and (b) overturning moment due to the presence of a square-cross-section wave barrier (calculated based on regression formulas obtained from Fig. 17 using H_{av} , H_s , and H_{\max} as input)

Table 7 Values of the wave height, wave period, base shear, and overturning moment extracted from the experiments conducted on the jacket with a wave barrier having a square cross section

Test ID	H (cm)				T (s)		F (kg)			M (kg.m)		
	H_{w-in}	H_{av}	H_s	H_{ma}	T_{w-in}	T_{av}	F_{av}	F_s	F_{\max}	M_{av}	M_s	M_{\max}
FN23	23	11.18	19.6	29.2	1.8	1.4	19.2	38.9	57.6			
FS23	23	10.02	16.1	25.0	1.8	1.4	17.7	31.5	43.4			
MN23	23	11.17	19.6	31.7	1.8	1.5				88.36	138.2	211.02
MS23	23	10.53	16.6	25.9	1.8	1.4				80.85	115.4	170.58

Table 8 The unknown coefficients of Eqs. (2)-(7) calculated based on the regression analysis of the data extracted from the experiments conducted on the jacket with a wave barrier having a square cross section

Test ID	Eq. (1)				Eq. (2)				Eq. (3)			
	a_1	b_1	R^2	$RMSE$	a_2	b_2	R^2	$RMSE$	a_3	b_3	R^2	$RMSE$
FN23	1.73	7.03	0.98	1.63	0.88	0.12	0.98	0.02	28.22	5.14	0.98	1.19
FS23	1.92	-0.34	0.98	1.17	0.97	-0.01	0.97	0.02	37.62	-0.32	0.98	1.01
Test ID	Eq. (4)				Eq. (5)				Eq. (6)			
	a'_1	b'_1	R^2	$RMSE$	a'_2	b'_2	R^2	$RMSE$	a'_3	b'_3	R^2	$RMSE$
MN23	7.27	-3.76	0.98	6.61	1.09	-0.01	0.98	0.03	1066.00	-24.19	0.98	42.52
MS23	7.76	-12.47	0.97	6.50	1.18	-0.07	0.97	0.03	1301.01	-101.40	0.98	52.93

Table 9 The percentage of decrease in the base shear and overturning moment due to the presence of a wave barrier having a square cross section

Decrease of base shear (%)			Decrease of overturning moment (%)		
Mean	Significant	Maximum	Mean	Significant	Maximum
8.57	18.97	24.67	9.29	19.78	23.71

4. Conclusions

The effects of a floating wave barrier installed in front of an offshore jacket structure on the wave height and jacket’s base shear and overturning moment were experimentally investigated. A jacket model with the height of 4.55 m was fabricated and tested in wave flume of NIMALA marine laboratory. A square cross section was selected for the wave barrier. Results showed that the average decrease in the jacket’s base shear due to the presence of a floating wave barrier with square cross section was 18.97%. The use of the wave barriers with square cross section also resulted in 19.78% decrease in the jacket’s overturning moment. Hence, it can be concluded that a wave barrier can significantly reduce the base shear and overturning moment in an offshore jacket structure.

Acknowledgements

The authors would like to thank the technical staff of NIMALA marine laboratory specially Eng. Taghi Aliakbari and Eng. Seyyed Abolfazl Hashemi. The support from the Vice-chancellery for Research and Technology of Islamic Azad University-Maragheh Branch is also highly appreciated. Useful comments of anonymous reviewers on draft version of the paper are also highly appreciated.

References

Abul-Azm, A.G. and Gesraha M.R. (2000), “Approximation to the hydrodynamics of floating pontoons under oblique waves”, *Ocean Eng.*, 27, 65-84. [https://doi.org/10.1016/S0029-8018\(98\)00057-2](https://doi.org/10.1016/S0029-8018(98)00057-2).
 Asgari Motlagh, A., Shabakhty, N. and Kaveh, A. (2021), “Design optimization of jacket offshore platform considering fatigue damage using Genetic Algorithm”, *Ocean Eng.*, 227, 27-30.

- <https://doi.org/10.1016/j.oceaneng.2021.108869>.
- Chakrabarty, S.K. (2005), "Handbook of Offshore Engineering", San Francisco.
- Chan, E.S., Cheong, H.F. and Tan, B.C. (1995), "Laboratory study of plunging wave impacts on vertical cylinders", *Offshore Eng.*, **1**(2), 94-100. <https://doi.org/10.1016/j.oceaneng.2020.107191>.
- Christensen, E.D., Bingham, H.B., Skou Friis, A.P., Larsen, A.K. and Jensen, K.L. (2018), "An experimental and numerical study of floating breakwaters", *Coast. Eng.*, **137**, 43-58. <https://doi.org/10.1016/j.coastaleng.2018.03.002>.
- Dong, G.H., Zheng, Y.N., Li Y.C., Teng, B., Guan, C.T. and Lin, D.F. (2008), "Experiments on wave transmission coefficients of floating breakwaters", *Ocean Eng.*, **35**, 931-938. <https://doi.org/10.1016/j.oceaneng.2008.01.010>.
- Gesraha, M.R. (2006), "Analysis of shaped floating breakwater in oblique waves: I. Impervious rigid wave boards", *Appl. Ocean Res.*, **28**, 327-338. <https://doi.org/10.1016/j.apor.2007.01.002>
- Goda, Y., Haranka, S. and Kitahata, M. (1966), "Study on impulsive breaking wave forces on piles", Report of Port and Harbour Technical Research Institute, **6**(5), 1-30.
- Hildebrant, A. (2013), "Hydrodynamic of breaking waves on offshore wind turbine structures", Ph.D. Thesis, Institute for Hydraulics, Waterways, and Coastal Engineering, Leibniz University, Hanover, Germany.
- ITTC maneuvering group members, Testing and Extrapolation Methods (2008), Manoeuvrability Captive Model Test Procedures, ITTC– Recommended, 7.5 - 02 06 – 02, Revision 02.
- Ji, C.Y., Yang, K., Cheng, Y. and Yuan, Z.M. (2017), "Numerical and experimental investigation of hydrodynamic performance of a cylindrical dual pontoon-net floating breakwater", *Coast. Eng.*, **129**, 1-16. <https://doi.org/10.1016/j.coastaleng.2017.08.013>.
- Jusoh, I. (2021), "Base shear and overturning moment on jacket structure with marine growth", *Int. J. Eng. Trends Technol.*, **58**, 1-4. <https://doi.org/10.14445/22315381/IJETT-V58P202>.
- Morison, J.R., O'Brien, M.P., Johnson, J.W. and Schaaf, S.A. (1950), "The forces exerted by surface waves on piles", *J. Petroleum Technol.*, **2**(5), 149-154.
- MurgoitioEsandi, J., Buldakov, E., Simons, R. and Stagonas, D. (2020), "An experimental study on wave forces on a vertical cylinder due to spilling breaking and near-breaking wave groups", *Coast. Eng.*, **162**, 17-30. <https://doi.org/10.1016/j.coastaleng.2020.103778>.
- National Iranian Marine Laboratory (2018), <http://www.nimala.ir>.
- Nikpour, A.H., Moghim, M.N. and Badri, M.A. (2019), "Experimental study of wave attenuation in trapezoidal floating breakwaters", *China Ocean Eng.*, **33**, 103-113. <https://doi.org/10.1007/s13344-019-0011-y>, ISSN 0890-5487.
- Rahman, M.A., Mizutani, N. and Kawasaki, K. (2006), "Numerical modeling of dynamic responses and mooring forces of submerged floating breakwater", *Coast. Eng.*, **53**, 799-815. <https://doi.org/10.1016/j.coastaleng.2006.04.001>.
- Sannasiraj, S.A., Sundar, V. and Sundaravivelu, R. (1998), "Mooring forces and motion responses of pontoon-type floating breakwaters", *Ocean Eng.*, **25**, 27-48. [https://doi.org/10.1016/S0029-8018\(96\)00044-3](https://doi.org/10.1016/S0029-8018(96)00044-3).
- Sruthi, C. and Sriram, V. (2017), "Wave impact load on jacket structure in intermediate water depth", *Ocean Eng.*, **140**, 183-194. <https://doi.org/10.1016/j.oceaneng.2017.05.023>.
- Tsai, P.W., Alsaedi, A., Hayat, T. and Chen, C.W. (2016), "A novel control algorithm for interaction between surface waves and a permeable floating structure", *China Ocean Eng.*, **30**, 161-176. <https://doi.org/10.1007/s13344-016-0009-7>.
- Zhao, F.F., Kinoshita, T., Bao, W.G., Huang, L.Y., Liang, Z.L. and Wan, R. (2012), "Interaction between waves and an array of floating porous circular cylinders", *China Ocean Eng.*, **26**, 397-412. <https://doi.org/10.1007/s13344-017-0042-1>